Journal of
Materials Chemistry B

Accepted Manuscript

Volume 1 | Number 1 | Jan 2013 | Pages 1–100

Journal of
Materials Chemistry B

Materials for biology and medicine
www.rsc.org/materialsB

ROYAL SOCIETY
OF CHEMISTRY

ROYAL SOCIETY
OF CHEMISTRY

www.rsc.org/materialsB

Journal of Materials Chemistry B

Cite this: DOI: 10.1039/c0xx00000x

www.rsc.org/xxxxxx

PAPER

Tailoring Doxorubicin sustainable release from biopolymeric smart matrix by Congo Red as molecular helper

Valeria E. Bosio,[a] Azucena Gómez López,[b] Arup Mukherjee,[c] Magdalena Mechetti[b] and Guillermo R. Castro[a],*

Doxorubicin (Dox) was co-encapsulated with Congo Red (CR) in order to increase drug encapsulation and sustain the release from gel microbeads composed of Alginate-Carboxy Methyl Guar Gum (68/32) for oral controlled delivery. No release of both cargo molecules from the microbeads at pH 1.2 in 90 minutes was detected. However, 62 % CR and 16 % Dox were released from the gels at pH 7.4 at 37 °C in 8 hours when both the cargo molecules are alone. Presence of CR in the formulation reduces in about 25-30 % the release of Dox 10 under the same experimental conditions. Rheological properties of the formulations have been investigated at different temperatures between 20 and 37 ºC. Shear thinning behavior was observed by steady-shear flow experiments for all of them and no yield stress was observed for any of the formulations. The temperature effect on Alg-CMGG-Dox-CR evidenced a synergic action between Dox and CR. Dynamic frequency sweep tests were performed to study the viscoelastic properties of the formulations. The patterns observed for Alg-CMGG indicated physical gel characteristics; however all other formulations showed a typical behavior of concentrated solutions. These 15 results are confirming the interaction of Dox and CR and the positive effect on sustainable release in oral delivery.

Introduction

Bioactive molecules containing aromatic rings like anthracyclines (e.g. doxorubicin, etc...) are highly used in chemotherapies. 20 However, anthracyclines use to display undesirable side effects in patients such as congestive heart failure, dilated cardiopathy, dramatic decrease of myeloid cell-lineages, severe immune suppression, nephropathies, alopecia, etc. which are restricting their extensive therapeutic use. Formulations can modify many 25 parameters of drug release from kinetic to organs targeting, reducing drug toxicity and avoiding undesirable side effects. Several drugs/bioactive molecules were successfully encapsulated to improve bioavailability, bioactivity, controlled delivery and reduction of toxicity.[1] Micro- and nano-medicines 30 of dreadful diseases like cancer, AIDS, diabetes, cystic fibrosis, prion disease and tuberculosis are in different last trial phases of approval, and some of them are currently used in compassionate therapies.

35 [a] *Nanobiomaterials laboratory, Institute of Applied Biotechnology (CINDEFI, CONICET-UNLP, CCT La Plata), Dept. of Chemistry, School of Sciences, Universidad Nacional de La Plata, Calle 47 y 115. C.P. 1900 La Plata, Argentina. E-mail: grcastro@gmail.com*
[b] *Lab. de Física de Fluidos y Electrorreología, Depto. de Física, Facultad 40 de Ciencias Exactas y Tecnología, Universidad Nacional de Tucumán. Av. Roca 1800, (T4001MVB), Tucumán, Argentina. E-mail: mmechetti@herrera.unt.edu.ar*
[c] *Department of Chemical Technology, Calcutta University, 92, A.P.C. Road, Kolkata - 700009. India. E-mail: arupm1234@gmail.com*

45 Alternative formulations showing sustained molecular release properties depends on the choice of suitable carrier with expected high encapsulation efficiency, improved bioavailability and retention time, among other factors. The desired micro- and nano-medicines are generally formulated by hit and trial methods but 50 without rational. Polymer-based particles synthesized for controlled drug delivery could be an effective alternative to decrease the undesirable side effects.[2]

Galactomannans are neutral polysaccharides present in the seeds of some legumes, and consist of a mannan backbone (β-55 (1→4)-d-mannose) with α-D-galactose at C6. The mannose to galactose (M/G) ratio is dependent on the source of the galactomannan, and is 2:1 ratio for the Guar Gum (GG). The GG has five to eight times more stabilizing and thickening capacities than the starch, and is very required in food and pharmaceutical 60 industries.[3, 4] Also, the use of guar gum derivatives and blends were postulated as matrices for the encapsulation of drugs.[5, 6]

Alginates are linear biopolymers composed of beta-mannuronic acid (M units) and alpha-guluronic acid (G units) linked by 1–4 bonds with pKa of 3.38 and 3.65 respectively. 65 Alginate gelation is due to the stacking of the G units by ionotropic mechanism in presence of multivalent cations, e.g. Calcium, which cooperatively interact forming ionic bridges between different polymer chains. Alginate gels are showing structure commonly known as "egg box" by analogy with egg 70 containers. In between two crosslinking points, the mannuronic (M) units remain mostly free and the degree of ionization of carboxylate residues depends on external pH. At pH 1.2, the carboxylate of M unit is in the acid form (non-polar form, pKa 3.38). Meanwhile at pHs higher than 3.38, the M carboxylate 75 residue remains as anionic form. Additionally, alginate gels are unstable in the presence of cation-chelating agents such as phosphate or citric acid and/or competing non-gelling cations such as sodium or potassium which are present in biological fluids.[2, 7-9]

Another well-known biopolymer used in foods is pectin, a water-soluble polysaccharide, which is not degraded by the intestinal enzymes but can be hydrolyzed by the intestinal flora. Pectins (Pecs) are structural polysaccharides composed of linear
5 galacturonic acid methylates. Pecs from plant cell walls can be grouped as low-methoxylated (LMP), medium-methoxylated (MMP) and high-methoxylated pectins (HMPs) dependent upon individual esterification degree (ED). LM and MM pectins can be gelled easily by multivalent cations and HMP at acid pH plus
10 some solute.[10] Alg and Pec gels have been used earlier as a matrix for entrapment of molecules and cells in tissue engineering studies. Different gelled matrix, like films, particles and coated structures were also developed from these biopolymers following inotropic gelation for many applications.[2, 10, 11]

15 However, several factors must be taken into account for the development of drug micro- and nano-formulations. Among them, control on drug release kinetics, formulation environment, matrix-cargo interactions, effect of the environment in the formulation, and drug stability in the formulation. The new
20 capabilities of micro-devices are also influenced by particle size, surface charge, and the distribution ratio of hydrophobic/hydrophilic patches and pockets in the carrier system.[8] Rheological properties influence each step of such pharmaceutical processing. Matrix rheologies further affect the
25 release profile and formulation behavior along the gastrointestinal tract.[11, 12]

Doxorubicin hydrochloride (Dox) is commonly used in the treatment of many solid tumors, such as breast, lung, stomach and ovarian cancer. Dox inhibits cell growth by DNA intercalation
30 and inhibition of topoisomerase II. Unfortunately, Dox is highly toxic, by biodistribution to non-targeted tissues causing severe side effects, which are limiting this anthracycline molecule dosage and widespread applications. Therefore, new formulation strategies via Dox encapsulation into particulate drug delivery
35 systems are required to be developed. Generally, drug encapsulation offers many advantages, such as: (i) the protection of the drug against *in vivo* degradation, (ii) the reduction of potential toxic side effects associated with the drug doses, (iii) the increase in patient comfort by avoiding repetitive bolus injection
40 or the use of perfusion pumps, and (iv) the improvement in drug pharmacokinetics. Many studies have been carried out with doxorubicin, giving rise to various Dox-containing micro- or nano-particles such as polymeric carriers, inorganic magnetic nanoparticles where Dox is adsorbed onto their surface or even
45 solid lipid nanoparticles containing Dox as an ion-pair complex. Besides, the main challenge of the therapeutic molecules remains the entrapping of Dox with a high encapsulation rate and yield into such micro- and/or nano-particulate systems with high shelf-life stability, and established kinetic release. Also, the main
50 difficulties arise in controlling the molecular release, while also to find a compromise between encapsulation efficiency, drug leakage induced by diffusion and/or by matrix degradation, the biocompatibility and biodegradation of particle components and the formulation processes.[2, 11, 14]

55 Congo Red (CR) is an anionic secondary diazo dye with planar aromatic structure commonly used as an acid-base indicator, soluble in many solvents, but yields red colloidal fluorescent solutions in aqueous media made by stacking mechanism similarly to many aromatic drugs. The postulated
60 mechanism for CR aggregation is by hydrophobic interaction involving the π-π bonds of the aromatic rings making planar structures.[15] Additionally, CR was used to detect fibril proteins enriched in β sheet conformation useful in histological studies of some neurodegenerative pathologies such as Alzheimer's,
65 Creutzfeldt–Jacob's, Huntington's and Parkinson's diseases.[16] In previous work of our laboratory, CR was studied as molecular cargo in Alg-CMGG gel blends with different compositions. CR release studies were performed under many experimental conditions and the interaction between the cargo and the matrix
70 analyzed by vibrational spectroscopy.[4]

The aim of the present work is to tailor Dox loading and release from the Alginate-Carboxy Methyl Guar Gum microbead hydrogels with the use of CR as molecular helper. Kinetic studies of Dox release from the microbeads were performed *in-vitro* at
75 different pHs in presence or absence of CR. Interaction of matrix components were analyzed by rheological studies between 20 to 40 °C and complemented with vibrational spectroscopy studies.

Experimental

80 *Reagents*

Congo Red (CR), the sodium salt of benzidinediazo-bis-1-naphthylamine-4-sulfonic acid ($C_{32}H_{22}N_6Na_2O_6S_2$, MW: 696.66 g/mol, purity > 99%), was purchased from Merck (AG. Darmstadt). Doxorubicin (Dox) was a gift from LMK
85 pharmaceuticals (Buenos Aires, Argentina). Low viscosity sodium Alginate (Alg) (average Mη 1 x 10^5 Da) was obtained from Biochem S.A. (Buenos Aires, Argentina). Carboxy Methyl Guar Gum (CMGG) was received as a gift from Hindustan Gum and Chemicals Limited (India). All other reagents used were of
90 analytical grade purchased from Sigma (St. Louis, MO, USA) or Merck (Darmstadt, Germany). All the biopolymer and formulation solutions were made in MiliQ water (Millipore, Billerica, MA, USA). CR and Dox stock solutions (1.0 and 0.9 g/l respectively) and its dilutions were made in MiliQ water or
95 buffers.

Biopolymer formulations solutions

Simple biopolymer solutions of Alg (3.5 %, w/v) and CMGG (0.5 %, w/v) were made by the addition of a weighted mass of
100 each biopolymer in a certain volume of miliQ water.

Blend biopolymer solution of Alg-CMGG (3.5-0.5 %, w/v) was prepared by the addition of 50 mg of CMGG every 5 minutes up to a 0.5 % (w/v) concentration in an Alg 3.5 % (w/v) solution.

Formulations of Alg-CMGG-CR and Alg-CMGG-Dox
105 solutions were prepared by the slow addition of CR or CR and DOX in the Alg-CMGG solutions up to 0.2 % (w/v), and stirred overnight at room temperature.

Biopolymer and microsphere formation

110 Hydrogel microspheres were made by extrusion of the mixture through a 100 μm diameter syringe with a pump (Watson-Marlow, UK). Alg (3.5 %) and CMGG (0.5 %) solution with or without CR (0.2 %) and Dox (0.2 %) were dropped into a solution containing 50 mM $CaCl_2$ (0 ºC) under continuous stirring
115 in order to avoid coalescence of gel beads. Microspheres were aged in calcium chloride solution for 48 h, followed by filtration on paper (Whatman #1). Filtered microspheres were kept in solution containing 50 mM $CaCl_2$ and 10 μM NaN_3 at 5 °C. Alternatively, microspheres were lyophilized and/or air-dried at
120 room temperature and then stored as it was mentioned before.

Dox and Congo Red loading

Dox or CR entrapment efficiency was determined by dissolving 100 mg of microspheres in 5.0 ml containing 100 mM
125 sodium phosphate buffer (pH= 7.4), and centrifuged at 10,000 xg for 10 minutes (5 °C). CR was quantified spectrophotometrically at 498 nm and Dox by spectrofluorimetry at λ_{exc}= 454 nm and λ_{em}= 588 nm with an appropriate calibration curve (Beckman, CA, USA, o Perkin Elmer LS 50B, Japan). The loading efficiency
130 was evaluated as follow:

$$\mathrm{E.E._A} = \frac{[A]_t}{[A]_o} \qquad (1)$$

In where, $\mathrm{E.E._A}$ is the entrapment efficiency of the molecule A (Dox or CR); $[A]_o$, and $[A]_t$ are the supernatant concentrations of the molecule A at zero and t times respectively.

Dox and Congo Red kinetic release studies from Alg-CMGG microparticles

Release profiles from ALG-CMGG microspheres of Dox were studied *in-vitro* under simulated stomach (pH= 2.0) and intestine (pH= 7.4) conditions. In addition, non-chelating and chelating buffers were used to study and modeling the diffusion process in Dox and Dox-CR kinetic release profiles at pH= 7.4 and 37 ºC.

In-vitro Dox kinetic release under stomach condition were performed in Clark and Lubs (KCl-HCl) buffer at pH=1.2. Non-chelating conditions were tested in 50 mM HEPES buffer at physiological pH (7.4). Chelating conditions were performed in the presence of 10 mM PBS buffer (pH= 7.4), where phosphates groups are responsible for the Ca^{+2} complexation in solution.

Dehydrated spheres (200.0 mg) were weighted in an analytical scale (Adventurer Ohaus, precision 100 µg) and placed in a Reacti-road flask of 4.0 ml of capacity, with 1.0 ml of buffer solution for release studies as previously reported.[1]

Rheological Measurements

The rheological experiments were performed using a Physica MCR 301 Anton Paar Rheometer controlled with Paar Physica Rheo Plus software (Graz, Austria). All measurements were carried out using 43-mm parallel plate geometry (PP43/GLSN16497 measurements system) and a P-PTD120-SN80470786 accessory system (Peltier temperature control). The gap between parallel plates was 0.7 mm. To eliminate or minimize the influence of thixotropy, the samples were subjected to shear for 10 minutes at 50 s^{-1} gradient of deformation (conditions obtained by preliminary tests).

Steady-shear and Dynamic- shear rheology

For steady shear measurements, shear rates ranging from 0.1 to 300 s^{-1} were used and the resulting stress was recorded. This range cover the shear rates expected in the actual small intestine, around 31 to 117 s^{-1}, estimated using the Small Intestinal Model falling within the bounds of what would be the "zero" shear rate viscosity and the "infinitely large" shear rate viscosity (figure 6).[17] Although the temperature of interest was 37 ºC, as mentioned already, rheological measurements were carried out at four different temperatures between 20 and 37 ºC to study the influence of temperature on the viscosity of the formulations and to obtain the activation energy. All the measurements were carried out in triplicate.

Flow curves were obtained by an up-down-up steps program to confirm the time-independence nature of the formulations. The apparent viscosity, shear stress and shear rate were recorded. The Ostwald-de Waele model, equation 2, commonly referred to as the power law model, has been used because it gives a good description of fluid flow behavior in the shear rate range considered and because none of the formulations showed yield stress.

$$\sigma = \kappa\dot{\gamma}^n \qquad (2)$$

In this equation, σ is shear stress (Pa); K is consistency index (Pa.sn), is shear rate (s^{-1}); n is a dimensionless flow behaviour index (0 < n < 1 for pseudoplastic fluids).

An Arrhenius relationship, equation (3), was used to describe the influence of temperature on apparent viscosity η (Pa.s).

$$\eta = A\exp\left(\frac{E_a}{RT}\right) \qquad (3)$$

Where η (Pa.s) is the apparent viscosity at a determined shear rate; A is a fitting parameter (Pa.s); T (K), is temperature; Ea (kJ/mol), is the activation energy and R is the universal gas constant.

Small amplitude oscillatory shear flow was applied to investigate the viscoelastic response function such as the complex viscosity, storage modulus and loss modulus as a function of the frequency. A strain amplitude sweep (0.1 – 10.0 %) at a fixed frequency (f= 1.0 Hz) was performed to establish the linear viscoelasticity regime. Then, a frequency sweep between 0.01< ω < 100 rad/s was performed within the linear viscoelasticity domain for each sample.

FTIR analysis

Samples and blends were analyzed by Fourier transformed infrared spectroscopy (JASCO FT/IR- 4200). Pellets were prepared by mixing the samples at 5.0 % (w/w) with potassium bromide (KBr, Pike technologies, WI, USA) and scanned with background correction at 256 scan numbers, against a high energy ceramic source and DLATGS detector.

Results and Discussion

Dox loading and release studies

The study and characterization of the Alg-CMGG as a CR carrier for oral delivery (see Fig. 1 for microspheres size distribution and Table 1 and Fig. 2a for release profiles) has proved a substantial system for increased Dox molecules loading when compared with the other biopolymeric matrixes studied like pectin.[1]
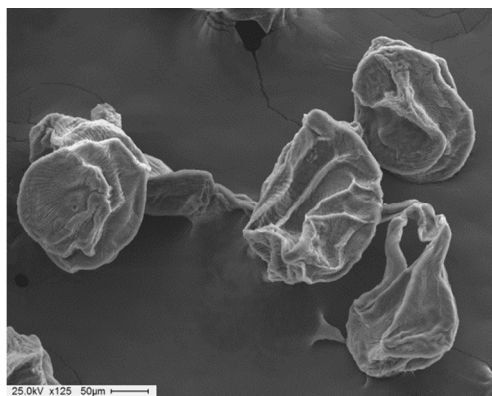

**Fig. 1** SEM microscopy of dehydrated Alg-CMGG microspheres

The Dox loading in Alg-CMGG matrix gel microspheres was 90 % (45 µg/mg of dry matrix), and 34 % higher than the loading on pectin with 55% of esterification degree (55 % PEC) microspheres.[1]

Studies of Dox release at 37 ºC in ALG-CMGG matrix gel microspheres under stomach simulated conditions (buffer Clark and Lubs, pH= 2.0) showed no drug release after 90 min

incubation. Meanwhile, Dox release at pH 7.4 under no chelating conditions was only 10 % after 8 hours at 37 ºC (Fig. 2b). However, Dox release at pH 7.4 under calcium-chelating conditions was approximately 16 %. These results are suggesting a stretched egg box structure effects on Alg-CMGG gel coacervate network due to calcium induced ionotropic gelation.
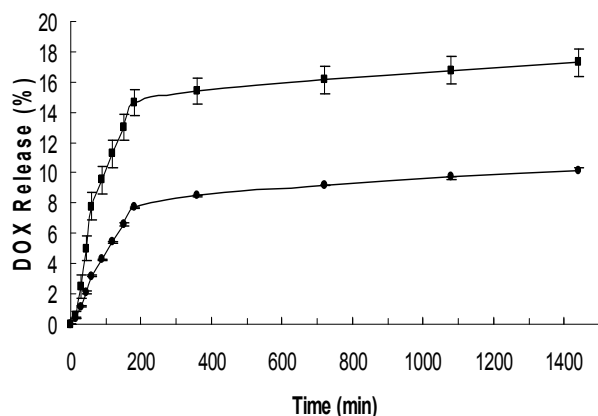
(a)
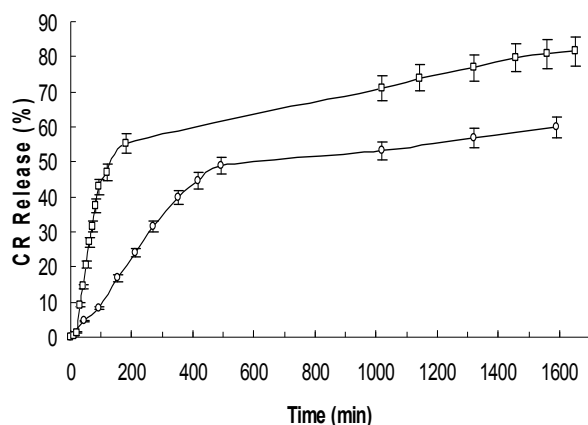
(b)

Fig. 2 (a) Congo Red kinetic release profile from ALG-CMGG microspheres at pH=7.4, in PBS (□) and HEPES (○) buffers and 37 °C. **(b)** Dox kinetic release profile from ALG-CMGG microspheres in PBS (■) and HEPES (●) buffers (pH=7.4) at 37 °C

Loading and release of Dox and CR studies in Alg-CMGG microspheres were carried out at 37 ºC (Fig. 3).

The Dox loading capability of the matrix in the presence of CR was increased in 34 % and 7 % respects to the Pec and Alg-CMGG without CR respectively (Table 1). In both release profiles the maximum percentages were founded below the previous values for the separated studies. Release of Dox and CR molecules from the microspheres with both loaded molecules at 37 ºC were 7 and 1 % under non-chelating conditions, while values of 12 and 2 % were founded under chelating conditions respectively (Table 1 and Fig. 3). For both molecules no changes on drug release under the stomach conditions compared with separated release profiles were observed.
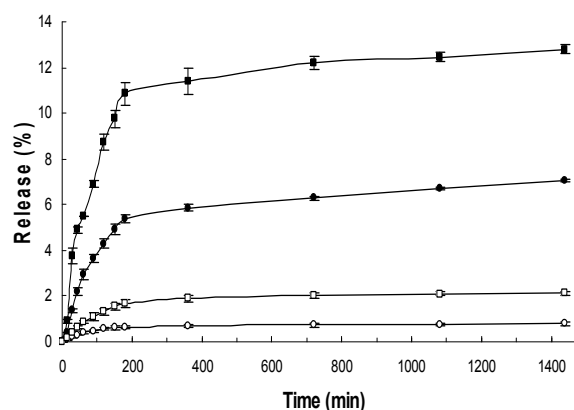

Fig. 3 CR and Dox kinetic release profile from Alg-CMGG microspheres loaded with Dox (black symbols) and CR (empty symbols) at 37 °C and pH=7.4, buffer PBS (squares) and HEPES (circles).

Table 1 Doxorubicin molecular loading and release characteristics from Alg-CMGG (7:1) in presence or absence of Congo Red at 37 ºC (three first columns) and Congo Red loading and release from of Alg-CMGG (7:1) in absence of Doxorubicin (last column).

Matrix	ALG-CMGG (7:1)				
Formulation	DOX	DOX (CR)	CR (Dox)	CR	Incubation Time (min)
Loading (%)	90	97	100	100	
Release (%), at pH (buffer)					
1.2 (Clark &Lubs)	0	0	0	0	90
7.4 (HEPES)	10	7	1	62	480
7.4 (PBS)	16	12	2	48	480

Dox release from the loaded study system showed a drastic decrease at pH 7.4 which can be associated due to interactions with the CR present in the matrix. From structural point of view both molecules contains aromatic rings, but the incidence of polar groups makes the big difference in the Dox and the CR behavior. The partition coefficient, log P, defined as the ratio of molecule concentration between n-octanol and water can be used as an indicator for compound hydrophilicity. The log P for Dox is 1.27 and for CR is 0.328 indicating low and high hydrophylicity for Dox and CR respectively. At pH 7.4 in both buffers the release of the Dox is reduced in about 25-30 % by the presence of CR, indicating an associative interaction probably made by the hydrophobic planar π-π aromatic structures.

The hypothesis of CR-Dox interaction is in agreement with the decrease of Dox release profile showed in profiles of figure 3. Also, the results are showing the relevance of matrix composition on Dox release during a possible synergism process. In this way, the results shown in figure 3 are indicating that both molecules are stable at least for 8 hours under our experimental conditions.

Rheology

The flow curves showed shear thinning behaviour and none of the samples showed yield stress. The smallest shear stress values were found for Alg-CMGG-CR (figure 4c)). This result
5 can also be observed for the apparent viscosity behaviour with the shear rate, Figure 6. In addition, a decrease in the shear stress values was observed at higher temperatures for Alg-CMGG-DOX-CR, Alg-CMGG-Dox and Alg-CMGG samples (figures 4a, 4b and 4d) except for Alg-CMGG-CR formulation (figure 4c)
10 showing an anomalous behaviour of shear stress and viscosity (figure 6) with temperature (increasing temperatures in the considered range, leads to increasing values of shear stress and viscosity).
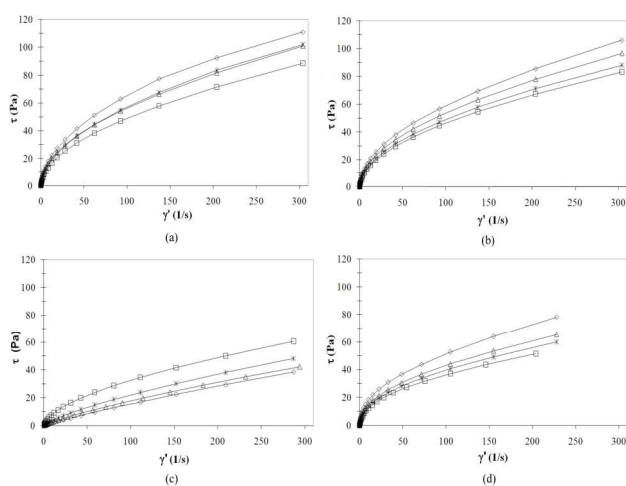

15 **Fig. 4** Flow curves for Alg-CMGG with Dox added, CR, or both at different temperatures. **(a)** Alg-CMGG-Dox-CR; **(b)** Alg-CMGG-Dox; **(c)** Alg-CMGG-CR; **(d)** Alg-CMGG. Symbols: ◊ 20 °C; Δ 25 °C; ＊ 30 °C; □ 37 °C

20

These results are suggesting strong interaction amongst CR and the biopolymeric matrix Alg-CMGG which can be attributed to the aromatic motif of the dye with hydrophobic pocket regions of Alginate, as vibrational spectroscopies revealed.[4] However the
25 addition of Dox and CR to Alg-CMGG, to give the Alg-CMGG-Dox-CR formulation, eliminates this anomalous behaviour with temperature.
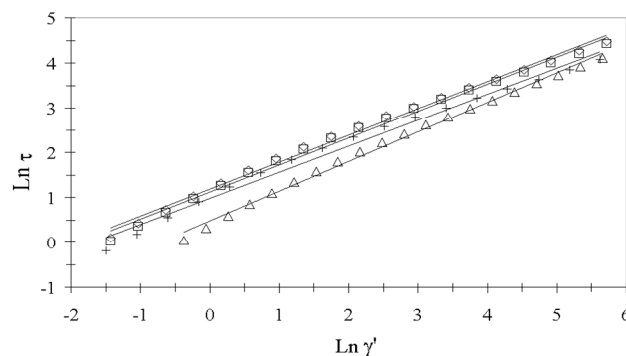

30 **Fig 5** Natural log curves of shear stress (Pa) vs shear rate (1/s) at 37 °C. symbols: ◊ Alg-CMGG-Dox-CR., □ Alg-CMGG-Dox, Δ Alg-CMGG-CR, ＋ Alg-CMGG

Natural log curves of shear stress against shear rate are
35 plotted in figure 5. The curves for all temperatures were fitted using the *power law* model and the rheological parameters obtained for all samples are shown in Table 2.

The power law model fitted the experimental data well. As can be seen in Table 2, the shear thinning behaviour of Alg-
40 CMGG and Alg-CMGG-Dox was greater (lowest values of flow index *n*) than Alg-CMGG-CR and Alg-CMGG-Dox-CR formulations. Lower values for the flow behaviour index (*n*) implied a greater decrease in the apparent viscosity at increased shear rates. These results can be attributed to particle aggregation
45 and greater orientation of the movement. The value of *n* in general for Alg-CMGG and Alg-CMGG-Dox was found to increase with the increase in temperature indicating decreasing pseudoplasticity. However for Alg-CMGG-CR sample the flow index decrease with the increase in temperature showing the
50 anomalous behaviour prior mentioned. In the case of Alg-CMGG-Dox-CR solution, the flow index was almost independent of temperature.

Table 2 H-B model rheological parameters for Alg, CMGG, Alg-
55 CMGG, Alg-CMGG-Dox, Alg-CMGG-CR and Alg-CMGG-Dox-CR at different temperatures

Formulations	T (°C)	K (Pa.s^n)	n	R^2
Alg-CMGG	20	4.40	0.55	0.99
	25	3.22	0.57	0.99
	30	2.78	0.58	0.99
	37	2.66	0.58	0.99
Alg-CMGG-Dox	20	3.91	0.59	0.99
	25	3.58	0.59	0.99
	30	3.09	0.61	0.99
	37	3.08	0.60	0.99
Alg-CMGG-CR	20	0.26	0.88	0.99
	25	0.31	0.87	0.99
	30	0.53	0.80	0.99
	37	1.63	0.65	0.99
Alg-CMGG-Dox-CR	20	3.60	0.62	0.99
	25	3.43	0.62	0.99
	30	3.40	0.61	0.99
	37	3.30	0.59	0.99

The consistency index *K* is a rheological parameter that reflects the values of the viscosity. This parameter showed a
60 greater temperature dependence for the Alg-CMGG blend than for the other formulations which can be attributed predominantly to the galactomannan. Figure 6 shows the changes in viscosity with increasing shear rate at 30 and 37 ºC (data for 20 and 25 ºC are not shown here). All formulations exhibited a shear-thinning
65 behaviour (in where apparent viscosity of solutions diminished with an increase in shear rate).

Addition of CR to the Alg-CMGG blend reduces the relative apparent viscosity at all temperatures considered, suggesting strong interaction amongst CR and Alg-CMGG solution. This
70 does not happen with the incorporation of Dox to Alg-CMGG in which case the curve at 20 ºC (not shown here) for Alg-CMGG-Dox is below that of Alg-Dox, almost superimposed at 25 ºC (not

shown here) but at 30 and 37 ºC the incorporation of Dox to Alg-CMGG increases the relative viscosity. At lower shear rates (1st Newtonian plateau and shear-thinning region), most of the samples showed a considerable decrease in apparent viscosity with the increase in temperature as can be seen with the exception of the Alg-CMGG-CR formulation that presents the inverse behaviour as already mentioned before. However, at high shear rates (2nd Newtonian plateau) the curves almost coincide with each other. The Alg-CMGG-Dox-CR presents in all cases the highest viscosity values and regarding the temperature effect, the positive interaction of CR and Dox in the selected matrix influences less significant compared with the other formulations.
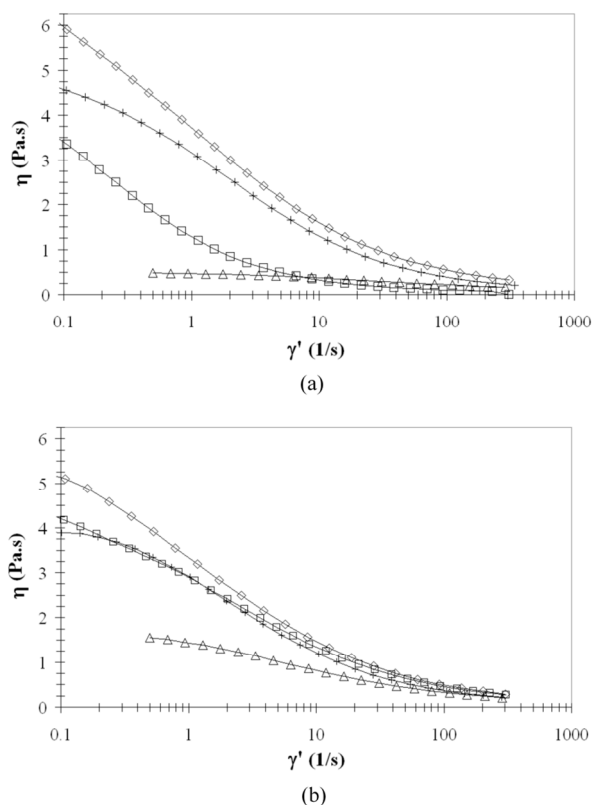

(a)

(b)

15 **Fig. 6** Apparent viscosity (Pa.s) vs shear rate for all samples at 30 °C. **(a)** and 37 °C. **(b)** Symbols: ◊, Alg-CMGG-Dox-CR; □, Alg-CMGG-Dox; Δ, Alg-CMGG-CR; +, Alg-CMGG.

The non-linear Arrhenius model (Equation 2) was used to fit 20 the data for apparent viscosity as a function of 1/T, to determine the activation energy of the proposed formulation Alg-CMGG-Dox-CR. The activation energy of this system decreased with the increase in shear rate and showed a maximum value at the start of the Newtonian plateau decreasing substantially with an increase 25 in shear rate, which is strictly related to the decrease in network density [15] and showed a considerably reduction in about one half with an increase in shear rate with values ranking from 22.42 KJ/mol (γ= 0.53 1/s) to 11.63 KJ/mol (γ= 92 1/s).

To study the viscoelastic behaviour of the formulations, 30 dynamic frequency sweeps tests were performed. The dynamic moduli, G' (Pa) and G'' (Pa) as a function of frequency (rad/s)

are plotted in figure 7. The storage modulus values G' were always greater than the loss modulus G'' for Alg-CMGG in the frequency range considered. This pattern is characteristic of weak 35 gel-like behaviour flow indicating a dominance of the elastic properties over viscous.[18] Instead the Alg-CMGG-Dox, Alg-CMGG-CR and Alg-CMGG-Dox-CR solutions showed a typical behaviour of concentrated solutions, which means that viscous flow predominate over the elastic response at low frequencies.[19] 40 It can be interpreted as that at low frequencies there was enough time for entanglement to occur and be disrupted during the oscillation period, which allowed viscous flow to predominate over the elastic character. However, for increasing frequencies the elastic character exceeds the viscous flow. In this situation the 45 sample acts as a crosslinked network and the result is G'> G".
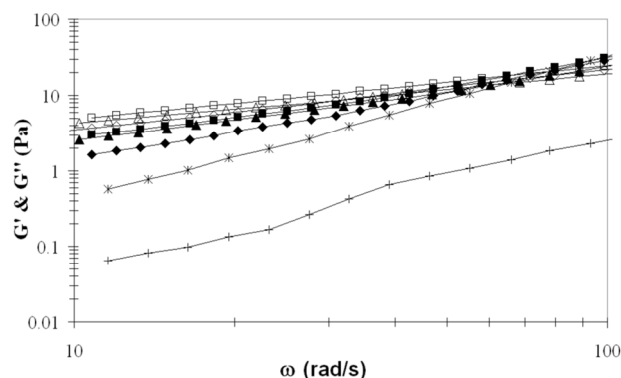

Fig. 7 Dynamic moduli as a function of frequency for Alg-CMGG-Dox-CR; Alg-CMGG-Dox; Alg-CMGG-CR and Alg-CMGG at 37ºC. 50 Symbols: ♦, G' and ◊, G'', Alg-CMGG-Dox-CR; ■,G' and □, G'', Alg-CMGG-Dox; ▲, G' and Δ, G'', Alg-CMGG-CR; ✳, G' and +, G'', Alg-CMGG.

The inverse of the crossover frequency can be seen as a 55 characteristic time, while the value of the modulus at the crossover point is a measure for the characteristic strength of the relaxation spectrum.[20] The crossover frequency of Alg-CMGG-Dox-CR is ω= 64.72 rad/s and the moduli value is 15.9 Pa in between 18.1 Pa for Alg-CMGG-Dox and 13.7 Pa for Alg-60 CMGG-CR. The loss tangent (tan δ= G''/G') indicates the relative contribution of elastic and viscous components to the rheological properties of a material. It can be see that for the formulations tan δ shows values greater than unity at low frequencies, decreasing to below unity with the increase in frequency. The decrease in tan 65 δ with an increase in frequency indicated that the system was in the pre-gel regime.[21]

FTIR analysis

Analysis of blend matrices containing Dox and CR were 70 performed by FTIR to determine type of interaction.

Displacement of at least four-five bands in the Dox-Alg-CMGG and CR-Alg-CMGG were observed (Table 3).

In the case of Dox, changes on FTIR assigned bending bands of (N-H), (O-H) groups, and stretching bands of (C-H, (–COOH), 75 and (φ=O) groups were observed as a result of matrix-cargo

interaction. In the case of CR, stretching bands were affected by the interaction of the dye with the matrix. However, those results are not able to justify the kinetic and rheological results Dox-CR cargos with the matrix.

Table 3 Major FTIR spectroscopic peaks assignments for Dox and CR free molecules and encapsulated into ALG-CMGG matrix

Wavenumbers (cm^{-1})		$\Delta\upsilon$ (cm^{-1})	Assignments
Free cargo molecules	In the Matrix		
Dox			
3389	3398	+9	δ (N–H)
3330	3340	+10	δ (H–O)
2932	2942	+10	σ (C–H)
1615	1614 and **1623**	+8	δ (N–H), ν(–COOH), ν(ϕ=O) and phenyl breathing modes
CR			
1453	1463sh	+10	ν(N=N)
1353, 1332	1362, 1341	+9, 9	Naphtyl ring
1279	1275sh, 1285sh	~ 5	ν(ϕ–ϕ)
1155	1165sh, 1178	~ 22	ν(ϕ–N)azo

FTIR experiments to determine the interaction of Dox with CR was performed (Table 4). Strong displacement of Dox stretching bands of C=O of ketone and aromatic ring and C-H group, also for benzene, C-O-CH$_3$ were observed. For CR, the displaced bands were assigned to (N=N), napthyl and (ϕ–ϕ) stretching bands. It can be speculated that Dox amino (-NH$_2$) groups can also form a strong hydrogen bridge interaction with polar groups of CR (i.e. sulfonate (-SO3) groups) when both molecules are located in the hydrophobic pockets of the matrix.

Additionally, CR phenyl ring and naphtyl ring structures can form strong π–π stacking interaction with the aromatic structure of Dox.

Table 4 FTIR spectroscopic peaks assignments for Dox and CR interaction

Wavenumbers (cm^{-1})		$\Delta\upsilon$ (cm^{-1})	Assignments
Free cargo molecules	Molecular Interaction		
Dox			
2932	2976	+44	ν (C=O) of ketone and quinine, σ (C–H)
1616	1614 and **1621**	+5	δ (N–H), ν(–COOH), ν(ϕ=O) and phenyl breathing modes
1579	1585	+6	Benzene ring, ν (C–O–CH$_3$)
1076	1067	-9	ν (C=O) of ketone and quinine
CR			
1418	1409	-9	ν(N=N)
1047	1042	-5	ν(ϕ–ϕ)

CR is able to form micelar solutions in aqueous solutions, because of low solubility (log P= 0.328), and stacking is an observed common phenomenon for hydrophobic aromatic molecules (Skowronek, et al., 1998). The Dox-CR stacking of hypothesis is also supported by experimental results of the kinetic release experiments, and the rheological curves and the modelling.

Conclusions

In the present work, tailoring of Alg-CMGG blend by the presence of Congo Red as helper molecule was demonstrated useful to encapsulate and control Doxorubicin release. First, no changes on Alg-CMGG gel microbeads stability in presence of Dox and Dox-CR were observed. Second, Dox encapsulation in Alg-CMGG gel microbeads increased in more than 26 % in presence of CR and the Dox release profiles from the matrix decreased 40%.

The alginate "egg-box" structure made by the calcium crosslinking on G units is also generating hydrophobic pockets of free M units at acid pH helping the cargoes, eg. CR and Dox, entrapped inside. At alkaline pHs, all carboxylic residues of alginate are negatively charged and the gel structure is destabilized showing swelling phenomenon by the diffusion of nonovalent ions (e.g. K^{1+}, Na^{1+}) from the solution to inside the gel matrix which are competing with the calcium crosslinker. The observed swelling effect is stronger in presence of phosphate by the quelating activity of the anion over calcium ions.

Another advantage is the time required to reach the plateau zone during the Dox release process which was more than 5 times slower under simulated intestinal conditions, meanwhile Alg-CMGG coacervate microspheres showed excellent stability at acid pH in where can be preserved with cargo release to the medium. The slow release of Dox from the microspheres at pH 7.4 allows controlling the cargo delivery and demonstrating the advantage of encapsulation in Alg-CMGG-RC to reduce the risk of molecular stacking favoring Dox biodisponibility and reducing the initial values of charge in the carriers. These results are suggesting a synergism between CR and Dox cargo molecules inside the Alg-CMGG matrix which allow to change the CR concentration in order to establish a proper Dox release kinetic.

Rheological studies of the Alg-CMGG-CR solutions showed a complex behavior: the viscosity decreased below 24 °C, but on the contrary increases from 24 to 40 °C. This fact seems to be advantageous since the ionotropic matrix gelation process is depending of the diffusion of the crosslinker, calcium ion. On the other side, a fast gelation is able to reduce the diffusion of the cargo, Dox, from the inner layers of the microbeads to the outside. Meanwhile, the viscosity of Alg-CMGG-Dox gradually increase with the temperature: at 25 °C is similar to the blend without the drug; however the viscosities at 30 and 37 °C are higher than the blend. High viscosities of Alg-CMGG-RC solutions containing Dox compared with the matrix alone were observed at all tested temperatures.

Vibrational spectroscopy of Dox and CR confirmed the interaction between the two molecules and low interaction with the matrix components. Presence of Congo Red in the matrix enhance the π-π aromatic hydrophobic interaction between the two cargo molecules.

Experiments of Dox kinetic release, rheological analysis of the formulation and vibrational spectroscopy are converging over the advantages of having CR as molecular helper in the Alg-

CMGG formulation matrix for Dox controlled release purposes. Also, the experiments allow to speculate over the kinetic and Dox concentration which can be modeled base on matrix composition and CR concentration. Experiments in cell cultures and Dox-CR intracellular tracking studies are now under study in our laboratory.

Notes and References

1 V. E. Bosio, M. V. Machain, A. Gómez López, I.O. Pérez De Berti, S.G. Marchetti, M. Mechetti, G.R. Castro, *Appl. Biochem. Biotechnol.*, 2012, **167**, 1365.

2 G. R. Castro, E. Bora, B. Panilaitis, D. L. Kaplan, in *Degradable Polymers and Materials*, ed. K. Khemani and C. Scholz, American Chemical Society Symposium Series № 939, Oxford University Press, Washington, 2006, p. 14.

3 I. Roy, M. Sardar, M. N. Gupta, *Biochem. Eng. J.*, 2005, **23**, 193.

4 V. E. Bosio, S. Basu, E. Chacon, J. A. Guida, A. Mukherjee, G. R. Castro, *React. Funct. Polym., 2014, in press*.

5 S. K. Bajpai, S. K. Saxena, S. Sharma, *React Funct. Polym.*, 2006, **66**, 659.

6 M. George, T. E. Abraham, *Int. J. Pharm.*, 2007, **335**, 123.

7 O. Smidsrød, G. Skjåk-Bráek, *Trends Biotechnol*. 1990, **8**, 71.

8 N. M. Velings and M. M. Mestdagh, *Polymer Gels and Networks*, 1995, **3**, 311.

9 S. K. Bajpai, S. Sharma, *React Funct Polym*, 2004, **59**, 129.

10. G.A. Islan, V. E. Bosio and G. R. Castro, *Macromol. Biosci.*, 2013, **13**, 1238.

11 W. B. Liechty, D. R. Kryscio, B. V. Slaughter, N. A. Peppas, *Ann. Rev. Chem. Biomol. Eng.,* 2010, **1**, 149.

12 T. Coviello, F. Alhaique, C. Parisi, P. Matricardi, G. Bocchinfuso, M. Grassi, *J. Control. Rel.*, 2005, **102**, 643.

13 H. Chi, V. Moturi, Y. Lee, *J. control. Rel.,* 2009, **136**, 88.

14 L. Zhu, V.P. Torchilin, *Integr. Biol.*, 2013,**5**, 96.

15 M. Skowronek, B. Stopa, L. Konieczny, J. Rybarska, B. Piekarska, E. Szneler, G. Bakalarski, I. Roterman, *Biopolymers*, 1998, **46**, 267.

16 P. Frid, S. V. Anisimov, N. Popovic, *Brain Res. Rev.*, 2007, **53**, 135.

17 A. Tharakan, in Modelling of physical and chemical processes in the small intestine *(PhD Thesis), University of Birminghan, UK.* p. 47.

18 R. Lapasin, S. Pricl, in *Rheological of industrial polysaccharides: Theory and applications*. Chapman & Hall, New York, 1995, p. 620.

19 S. B. Ross-Murphy, K. P. Shatwell, *Biorheology,* 1993, **30**, 217.

20 R. H. W. Wientjes, M. H. G., Duits, R. J. J. Jongschaap, J. Mellema, *Macromolecules,* 2000, **33**, 9594.

21 S. O. Shon, B. C. Ji, Y. A. Han, D. J. Park, I. S. Kim, J. H. Choi, *J. Appl. Polym. Sci.*, 2007, **104**, 1408.